Polynomial Chaos Approximation for Worst-case Transient Performance of Linear Systems

Mario Izquierdo Serra * **Maurice Martin** *
Simon Delchambre * **Stefan Winkler** * **Harald Pfifer** **

* *Airbus Defence and Space GmbH, Immenstaad am Bodensee, 88090, Germany (e-mail: {mario.izquierdo_serra, maurice.martin, simon.delchambre, stefan.st.winkler}@airbus.com).*
** *Chair of Flight Mechanics and Control, Technische Universität Dresden, Dresden, 01307, Germany (e-mail: harald.pfifer@tu-dresden.de)*

Abstract: The goal of this paper is to approximate the worst-case transient performance of uncertain linear time-invariant systems, subject to both $\mathcal{L}_2$-bounded input signals and known disturbances, e.g., reference tracking commands. System uncertainties are described through real-valued random variables with a known probability distribution. The worst-case performance analysis is formulated as a parametric Riccati differential equation, which is approximately solved using polynomial chaos expansion. The objective is to estimate a bound on the Euclidean norm of the system output at a given time. The effectiveness of the approach is demonstrated on the example of a spacecraft attitude and orbit control system.

Keywords: Uncertain systems, probabilistic robustness, guidance, navigation and control of aircraft and spacecraft

1. INTRODUCTION

This paper deals with the transient performance analysis of continuous linear time-invariant systems (LTI). These systems are subject to model uncertainties and disturbances that can cause its performance to deviate from its desired one. In particular, this paper focuses on LTI systems affected simultaneously by deterministic and $\mathcal{L}_2$-bounded input signals. The former ones include constant or time-varying inputs signals that are perfectly known at each point in time, e.g., reference commands or fully defined environmental disturbances. The latter ones cover unknown disturbances. The objective is to stochastically estimate the worst-case performance of these systems during their transient response. The Euclidean norm of the system output at a given time will be used as the performance metric. A wide range of engineering applications in the aerospace industry where the primary objective is performing a manoeuvre or tracking a predefined trajectory fall in this category, e.g., spacecraft acquisition sequence (Izquierdo Serra et al., 2025), unmanned aerial vehicles (Althoff et al., 2015), or entry vehicles trajectories (Derollez and Manchester, 2020).

This paper proposes an approximation of the worst-case transient performance of such LTI systems. To provide worst-case statements for this type of problem, the main idea in Thiele et al. (2025) is adapted in this paper to incorporate deterministic signals into the analysis. The novel approach in Thiele et al. (2025) introduces worst-case gain computations of uncertain linear time-varying (LTV) systems over a finite horizon subject to mixed disturbances. Through a state-space augmentation, our LTI system with deterministic and $\mathcal{L}_2$-bounded signals is reformulated as a finite-horizon LTV system that includes an additional state and considers only $\mathcal{L}_2$-bounded signals as inputs. Biertümpfel et al. (2023) also uses a similar state-space augmentation for the robustness analysis of nonlinear dynamic systems.

The robustness analysis of finite-horizon LTV systems is well-discussed in literature. Quadratic performance metrics of nominal LTV systems have well-defined solutions based on Riccati differential equations (RDEs), as shown in Green and Limebeer (1995). For uncertain LTV systems, robust quadratic performance metrics can be obtained by extending the nominal solutions resulting in parameter-dependent RDEs, see Biertümpfel and Pfifer (2018). A recent approach to approximate the solution of the parametric RDE based on polynomial chaos expansion (PCE) is proposed in Evangelisti and Pfifer (2022) and is used in this paper. Originally introduced in Wiener (1938), polynomial chaos is a series expansion similar to the Fourier series for periodic time signals. Evangelisti and Pfifer (2022) makes use of this theory to provide an approximation of the robust quadratic performance metrics.

Within the finite-horizon LTV framework, Schweidel et al. (2020) presents a method to compute worst-case disturbances for finite-horizon LTV systems with a non-zero initial condition. Farhood (2024) focuses on the robustness analysis of discrete-time uncertain LTV systems subject to uncertain initial conditions. A sampled-based approach is

developed in Derollez and Manchester (2020) to propagate the dynamics and uncertainties around the nominal trajectory of a Mars entry vehicle.

The approximated worst-case analysis methodology presented in this paper is applied to the attitude and orbit control system (AOCS) of an Earth observation satellite during an orbital manoeuvre. During this manoeuvre, the main boost engines are actuated resulting in torques on the spacecraft and a transient response on the spacecraft attitude. The manoeuvre is modelled as a deterministic input torque acting directly on the spacecraft. In addition, unknown external environmental disturbances are modelled as $\mathcal{L}_2$-bounded signals. The Euclidean norm of the spacecraft attitude needs to be assessed at given times during the transient response of the system.

2. PROBLEM STATEMENT

The mathematical formulation of the worst-case transient performance analysis of LTI systems subject to both deterministic and $\mathcal{L}_2$-bounded signals is presented here. Consider a LTI system G defined on $t \in [0, T]$ with finite time horizon $T < \infty$ subject to uncertain parameters δ of the following form:

$$\begin{aligned} \dot{x}(t,\delta) &= A(\delta)x(t,\delta) + B_d(\delta)d(t) + B_u(\delta)u(t) \\ y(t,\delta) &= C(\delta)x(t,\delta) + D_d(\delta)d(t) + D_u(\delta)u(t). \end{aligned} \tag{1}$$

Here, $x(0) = 0$, $x(t,\delta) \in \mathbb{R}^{n_x}$ is the state vector, $d(t) \in \mathbb{R}^{n_u}$ the deterministic input vector, $u \in \mathcal{L}^{n_u}_{2,[0,T]}$ the $\mathcal{L}_2$-bounded input vector, and $y(t,\delta) \in \mathbb{R}^{n_y}$ the output vector. The finite-horizon $\mathcal{L}_{2[0,T]}$ norm of the signal $u : [0,T] \to \mathbb{R}^{n_u}$ is defined as $\|u\|_{2,[0,T]} := \sqrt{\int_0^T u(t)^\top u(t) dt}$. Moreover, $\delta \in \Delta^{n_\delta} \subset \mathbb{R}^{n_\delta}$ is an unknown parameter vector, subject to a given probability distribution $p(\delta)$, where n_δ represents the number of uncertain parameters. A, B_d, B_u, C, D_d, and D_u are piecewise-continuous matrix functions, that map each Δ^{n_δ} to a real matrix of appropriate dimension. To simplify notation, this paper sometimes omits explicit time dependence, as it will be clear from context.

To assess the transient performance of (1), this paper will focus on the output Euclidean norm at a given time. This metric will be used to bound the set of outputs y at a given time T. The worst-case transient performance, with respect to the output y at a given time T of the system in (1) over all possible parameter and input perturbations is expressed as:

$$\sup_{\delta\in\Delta^{n_\delta}} \sup_{\substack{u\in\mathcal{L}_{2,[0,T]},\\ u\neq 0, x(0)=0}} \|y(T,\delta)\|_2 . \tag{2}$$

To provide worst-case statements of the metric in (2), a similar state-space augmentation as in Thiele et al. (2025) is applied to (1). The deterministic input disturbance d is multiplied by a constant driving term with value 1, which extends the state vector and pushes the term $B_d(\delta)d(t)$ into the state matrix. The resulting state-space representation is:

$$\begin{aligned} \begin{bmatrix} \dot{x} \\ 0 \end{bmatrix} &= \begin{bmatrix} A & B_d d \\ 0 & 0 \end{bmatrix} \begin{bmatrix} x \\ 1 \end{bmatrix} + \begin{bmatrix} B_u \\ 0 \end{bmatrix} u \\ y &= [C \;\; D_d d] \begin{bmatrix} x \\ 1 \end{bmatrix} + D_u u. \end{aligned} \tag{3}$$

The system (3) is identical to (1). Subsequently, the constant driving term is replaced with an additional state $x_d := 1$ providing the following augmented system:

$$\begin{aligned} \underbrace{\begin{bmatrix} \dot{x} \\ 0 \end{bmatrix}}_{\dot{\hat{x}}} &= \underbrace{\begin{bmatrix} A & B_d d \\ 0 & 0 \end{bmatrix}}_{\hat{A}} \underbrace{\begin{bmatrix} x \\ x_d \end{bmatrix}}_{\hat{x}} + \underbrace{\begin{bmatrix} B_u \\ 0 \end{bmatrix}}_{\hat{B}} u \\ y &= \underbrace{[C \;\; D_d d]}_{\hat{C}} \underbrace{\begin{bmatrix} x \\ x_d \end{bmatrix}}_{\hat{x}} + \underbrace{D_u}_{\hat{D}} u. \end{aligned} \tag{4}$$

The system (4) contains a non-zero initial condition of its additional state x_d. This state-space augmentation allows the inclusion of deterministic input signals in the finite-horizon robustness analysis framework.

3. BACKGROUND

3.1 Uncertain LTV Systems with Non-zero Initial Conditions

Consider a LTV system H defined on $t \in [0, T]$ with finite time horizon $T < \infty$ subject to uncertain parameters δ of the following form:

$$\begin{aligned} \dot{x}(t,\delta) &= A(t,\delta)x(t,\delta) + B(t,\delta)u(t) \\ y(t,\delta) &= C(t,\delta)x(t,\delta) + D(t,\delta)u(t), \end{aligned} \tag{5}$$

where $x(0) = x_0$. A, B, C, and D are piecewise-continuous matrix functions, that map each $[0,T] \times \Delta^{n_\delta}$ to a real matrix of appropriate dimension. Assume $D(T,\delta) = 0$ for all $\delta \in \Delta^{n_\delta}$.

Among the different performance metrics to analyse uncertain finite time horizon LTV systems, here we focus on the Euclidean norm of the system output y in (5). The worst-case output Euclidean norm at time T for (5) is defined as:

$$\sup_{\delta\in\Delta^{n_\delta}} \sup_{\substack{u\in\mathcal{L}_{2,[0,T]},\\ u\neq 0, x(0)=x_0}} \|y(T,\delta)\|_2 . \tag{6}$$

The following theorem, based on Moore (2015), provides an analysis condition to calculate an upper bound on the worst-case metric (6).

Theorem 1. Consider an uncertain LTV system defined by (5), with $x(0) = x_0$ and $\|u\|_{2,[0,T]} \leq b$. If there exists a scalar $a > 0$ and a continuous differentiable function $P(t,\delta) : [0,T] \times \Delta^{n_\delta} \to \mathbb{S}^{n_x}$ such that $P(T,\delta) = C^\top(T,\delta)C(T,\delta)$,

$$\dot{P}(t,\delta) = -\begin{bmatrix} I_{n_x} \\ P(t,\delta) \end{bmatrix}^\top E(t,\delta) \begin{bmatrix} I_{n_x} \\ P(t,\delta) \end{bmatrix}, \tag{7}$$

with the RDE coefficient matrix $E(t,\delta)$ defined as:

$$E(t,\delta) := \begin{bmatrix} E_{11}(t,\delta) & E_{12}(t,\delta) \\ E_{21}(t,\delta) & E_{22}(t,\delta) \end{bmatrix} = \begin{bmatrix} 0 & A^\top \\ A & BB^\top \end{bmatrix}, \tag{8}$$

and

$$\begin{bmatrix} x^\top(0)P(0,\delta)x(0) - a & 0 \\ 0 & a - \gamma^2 + b^2 \end{bmatrix} \leq 0, \tag{9}$$

then γ is an upper bound on (6). $\mathbb{S}^{n_x}$ describes the set of $n_x \times n_x$ symmetric matrices and I_{n_x} the identity matrix of order n_x.

Proof. The proof is omitted here for brevity. It requires minor modifications from the one given in Moore (2015).

3.2 PCE of Random Parameter-Dependent RDEs

Obtaining an upper bound on the worst-case gain (6) through Theorem 1 is computationally intractable, since existence of the solution $P(t,\delta)$ in (7) needs to be checked for all values of $\delta \in \Delta^{n_\delta}$. Evangelisti and Pfifer (2022) presents an alternative in the field of probabilistic robust control, making use of PCE to approximate the solution of parameter-dependent RDEs.

Polynomial chaos is an orthogonal series expansion used in the field of uncertainty quantification (Sullivan (2015)). The key idea behind PCE is to express $P(t,\delta)$ in (7) using appropriate orthogonal basis polynomials $\psi_\alpha : \Delta^{n_\delta} \to \mathbb{R}$:

$$P(t,\delta) = \sum_{\alpha=0}^{\infty} P_\alpha(t)\psi_\alpha(\delta). \tag{10}$$

Therein, $\alpha \in \mathbb{N}_0$, the P_α are time-variant deterministic expansion coefficients, and ψ_α are the orthogonal polynomials of degree α with respect to the probability density function of δ. Piprek (2020) shows that some polynomial families (e.g., Legendre, Hermite, Jacobi, etc.) are orthogonal with respect to some continuous probability density functions (e.g., uniform, Gaussian/normal, beta, etc.) and fulfil:

$$\begin{aligned} \psi_0 &= 1 \\ \langle \psi_\alpha, \psi_\beta \rangle &= \begin{cases} 0 & \text{if } \alpha \neq \beta \\ \mathbb{E}[\psi_\alpha^2] & \text{if } \alpha = \beta \end{cases} \qquad \forall \alpha, \beta \in \mathbb{N}_0, \end{aligned} \tag{11}$$

where $\langle \cdot, \cdot \rangle$ denotes the inner product:

$$\langle f, g \rangle = \mathbb{E}[fg] = \int_{\Delta^{n_\delta}} f(\delta)g(\delta)p(\delta)d\delta, \tag{12}$$

defined w.r.t. the probability density function $p(\delta)$.

The P_α coefficients are defined through the projection relation:

$$P_\alpha = \frac{\langle P(t,\cdot), \psi_\alpha \rangle}{\langle \psi_\alpha, \psi_\alpha \rangle} = \frac{\int_{\Delta^{n_\delta}} P(t,\delta)\psi_\alpha(\delta)p(\delta)d\delta}{\int_{\Delta^{n_\delta}} \psi_\alpha^2(\delta)p(\delta)d\delta}. \tag{13}$$

In practice, the infinite series in (10) needs to be truncated (see, e.g., Marelli and Sudret (2015)) as:

$$P(t,\delta) \approx \sum_{\alpha=0}^{L-1} P_\alpha(t)\psi_\alpha(\delta), \tag{14}$$

where the factor L represents the number of expansion coefficients and, for the total polynomial degree truncation scheme, is given by $L = \frac{(n_\delta + d_p)!}{n_\delta! d_p!}$, where d_p denotes the maximum total polynomial degree.

There exist several methods to compute the deterministic expansion coefficients P_α in (13). Evangelisti and Pfifer (2022) uses the Galerkin projection, which preserves the mathematical structure of the problem.

Projecting the RDE on a finite-dimensional polynomial basis leads to a coupled system of L deterministic RDEs. For a full mathematical description, see Evangelisti and Pfifer (2022). Due to the impossibility of finding an exact solution to the infinite-dimensional RDE (7), the Galerkin approach tries to approximate the solution by (14).

With symmetric E_{11} and E_{22}, and $E_{12} = E_{21}^\top$, define by $\mathcal{E}(t,\delta)$ the symmetric $\mathbb{R}^{n_x(L+1)\times n_x(L+1)}$-valued matrix:

$$\mathcal{E}(t,\delta) := \left[\begin{array}{c|ccc} E_{11} & E_{12}\psi_0 & \dots & E_{12}\psi_{L-1} \\ \hline E_{21}\psi_0 & E_{22}\psi_0\psi_0 & \dots & E_{22}\psi_0\psi_{L-1} \\ \vdots & \vdots & \ddots & \vdots \\ E_{21}\psi_{L-1} & E_{22}\psi_{L-1}\psi_0 & \dots & E_{22}\psi_{L-1}\psi_{L-1} \end{array}\right]. \tag{15}$$

The projection of (15) onto each ψ_α is denoted by

$$\mathcal{E}_\alpha(t) = \frac{1}{\langle \psi_\alpha^2 \rangle}\langle \psi_\alpha, \mathcal{E}(t,\cdot)\rangle. \tag{16}$$

The projected system of RDEs is then written as:

$$\begin{aligned} \dot{P}_\alpha(t) &= -\begin{bmatrix} I_{n_x} \\ P_0(t) \\ \vdots \\ P_{L-1}(t) \end{bmatrix}^\top \mathcal{E}_\alpha(t) \begin{bmatrix} I_{n_x} \\ P_0(t) \\ \vdots \\ P_{L-1}(t) \end{bmatrix} \\ P_\alpha(T) &= \frac{1}{\langle \psi_\alpha^2 \rangle}\langle \psi_\alpha, P(T,\cdot)\rangle \quad \forall \alpha = 0, \dots, L-1. \end{aligned} \tag{17}$$

Thus, the computational intractable, infinite-dimensional RDE (7) is reduced to L coupled RDEs (17), as shown in Evangelisti and Pfifer (2022). The expansion coefficients $P_\alpha(t)$ can then be obtained simply by numerical integration of (17) and then used to reconstruct the approximated solution $P(t,\delta)$ with (14).

4. APPROXIMATED WORST-CASE ANALYSIS USING POLYNOMIAL CHAOS

This section presents a novel formulation for the worst-case transient performance analysis of uncertain LTI systems under deterministic and $\mathcal{L}_2$-bounded disturbances like in (1). The following theorem, based on modifications of Theorem 2 in Thiele et al. (2025) and Theorem 1 in Biertümpfel et al. (2023), provides an analysis condition to bound (2). It makes use of the augmented state-space representation in (4).

Theorem 2. Consider an uncertain LTV system defined by (4), with $x(0) = 0$, $x_d = 1$, and $\|u\|_{2,[0,T]} \leq b$. Assume $\hat{D}(T,\delta) = 0$ for all $\delta \in \Delta^{n_\delta}$. If there exists a scalar $a > 0$ and a continuous differentiable function $P(t,\delta) = \begin{bmatrix} P_{11} & P_{12} \\ P_{12}^\top & P_{22} \end{bmatrix} : [0,T] \times \Delta^{n_\delta} \to \mathbb{S}^{n_x+1}$ such that $P(T,\delta) = \hat{C}^\top(T,\delta)\hat{C}(T,\delta)$,

$$\dot{P}(t,\delta) = -\begin{bmatrix} I_{n_{\hat{x}}} \\ P(t,\delta) \end{bmatrix}^\top E(t,\delta) \begin{bmatrix} I_{n_{\hat{x}}} \\ P(t,\delta) \end{bmatrix}, \tag{18}$$

with

$$E(t,\delta) = \begin{bmatrix} 0 & \hat{A}^\top \\ \hat{A} & \hat{B}\hat{B}^\top \end{bmatrix}, \tag{19}$$

and

$$\begin{bmatrix} P_{22}(0,\delta) - a & 0 \\ 0 & a - \gamma^2 + b^2 \end{bmatrix} \leq 0, \tag{20}$$

then γ is an upper bound on (2).

Following the same idea as in Thiele et al. (2025) and Biertümpfel et al. (2023), Theorem 2 divides P into a $n_x \times n_x$ matrix P_{11} (related to states x) and a scalar P_{22} (related to the additional state x_d).

Proof. The proof relies on the definition of an uncertain time-varying quadratic storage function $V(x,t,\delta) =$

$\hat{x}(t,\delta)^\top P(t,\delta)\hat{x}(t,\delta)$. After perturbing the RDE in (18) with an infinitesimal small positive scalar ϵ, the resulting Riccati differential inequality can be rewritten as a linear matrix inequality applying Schur's complement:

$$\begin{bmatrix} \dot{P} + P\hat{A} + \hat{A}^\top P & P\hat{B} \\ \hat{B}^\top P & -I_{n_u}(1-\epsilon) \end{bmatrix} \leq 0, \tag{21}$$

Left and right multiplying (21) with $\left[\hat{x}(t,\delta)^\top, u(t)^\top\right]$ and $\left[\hat{x}(t,\delta)^\top, u(t)^\top\right]^\top$, respectively yields

$$\underbrace{\hat{x}^\top \dot{P}\hat{x} + \hat{x}^\top P \overbrace{(\hat{A}\hat{x}+\hat{B}u)}^{\dot{\hat{x}}} + \overbrace{(\hat{x}^\top\hat{A}^\top + u^\top\hat{B}^\top)}^{\dot{\hat{x}}^\top} P\hat{x}}_{\dot{V}(x,t,\delta)} - (1-\epsilon)u^\top u \leq 0. \tag{22}$$

Integrating from 0 to T provides

$$\hat{x}^\top(T,\delta)P(T,\delta)\hat{x}(T,\delta) - \hat{x}^\top(0,\delta)P(0,\delta)\hat{x}(0,\delta) - (1-\epsilon)\underbrace{\int_0^T u^\top u dt}_{\|u\|^2_{2,[0,T]}} \leq 0. \tag{23}$$

Using (4) and the definition of $P(T,\delta)$ in Theorem 2 and recalling that $\hat{D}(T,\delta) = 0$, the first part of (23) results in

$$\hat{x}^\top(T,\delta)P(T,\delta)\hat{x}(T,\delta) = y^\top(T,\delta)y(T,\delta). \tag{24}$$

Recalling that $x(0) = 0$ and $x_d = 1$, the second term of (23) becomes

$$\hat{x}^\top(0,\delta)P(0,\delta)\hat{x}(0,\delta) = P_{22}(0,\delta). \tag{25}$$

From (23), (24), and (25), it follows that

$$\|y(T,\delta)\|_2^2 - P_{22}(0,\delta) - (1-\epsilon)\|u\|^2_{2,[0,T]} \leq 0. \tag{26}$$

Multiplying the left-hand-side of (20) with $[x_d, 1]$ and $[x_d, 1]^\top$, respectively results in

$$x_d^2 P_{22}(0,\delta) - a x_d^2 + a - \gamma^2 + b^2 \leq 0. \tag{27}$$

Recalling that $x_d = 1$, the inequality (26) can be substituted in (27) which yields the inequality

$$b^2 - (1-\epsilon)\|u\|^2_{2,[0,T]} + \|y(T,\delta)\|_2^2 - \gamma^2 \leq 0. \tag{28}$$

From the definition $\|u\|_{2,[0,T]} \leq b$, it can be concluded that $\|y(T,\delta)\|_2 \leq \gamma$.

4.1 Computational approach

For a given sample $\hat{\delta}_j$, Theorem 2 allows to obtain a bound γ on the Euclidean norm of the output y at time T of system (1). $P(T,\hat{\delta}_j)$ is used as the initial value to integrate backwards in time the RDE in (18). The RDE is integrated using the Matlab internal ODE solver *ode15s*. This solver is designed for stiff differential equations and, according to Biertümpfel and Pfifer (2018), performed best of all Matlab internal solvers for these type of problems. If a solution that stabilises the RDE is found, (20) is used to compute the bound γ.

Following Section 3.2, this paper expands the approach proposed in Evangelisti and Pfifer (2022) to this new class of problems. A polynomial chaos expansion is applied to approximate the solution $P(t,\delta)$ in (18), with the RDE coefficient matrix (19), yielding a coupled system of L deterministic RDEs. To solve the projected system of RDEs (17), it is necessary to compute the projection integrals (16) with (15) and the RDE coefficient matrix (19). In this paper, the required matrix projections (16) are computed by the linear fractional transformation (LFT) approach derived for uncertain matrices in Evangelisti and Pfifer (2024). This approach exploits the LFT structure (pre-separating the system into deterministic and stochastic components), leading to computational benefits.

If a solution to the coupled system of RDEs (17) is found for $[0,T]$, then the expansion coefficients of the lower right entry in $P_\alpha(t)$ are used to obtain the probability distribution of $P_{22}(0,\delta)$:

$$P_{22}(0,\delta) \approx \sum_{\alpha=0}^{L-1} P_{22,\alpha}(0)\psi_\alpha(\delta). \tag{29}$$

Using (29) and (20), a probability distribution of γ can be obtained, depending only on uncertainty vector δ and constants b and $P_{22,\alpha}(0)$. The probability distribution of γ is then sampled to estimate the probability distribution of the bound on $\|y(T,\delta)\|_2$. The methodology employed in this paper is summarized in Algorithm 1.

Algorithm 1 Probabilistic Worst-case Transient Performance Analysis based on RDE and PCE

1: **Input**: uncertain LTV system (1), $d(t)$, $\|u\|_{2,[0,T]} \leq b$, $\delta \in \Delta^{n_\delta}$ subject to $p(\delta)$, T, N_{samples}, d_p.
2: Build augmented system (4).
3: Compute L with d_p and n_δ.
4: Build projected RDE coefficient matrices (16) with (15) and (19).
5: Solve coupled system of RDEs (17) via backwards integration from T to 0.
6: **Output**: Solution $P_\alpha(t)$ $\forall\alpha = 0,\ldots,L-1$ and time vector t_{RDE} of the integration.
7: **if** t_{RDE} spans complete interval $[T,0]$ this means the coupled system of RDEs is solvable $\forall t \in [T,0]$ **then**
8: Extract $P_{22}(0,\delta)$ probability distribution from $P_\alpha(t)$ with (29).
9: Extract γ probability distribution from $P_{22}(0,\delta)$ probability distribution and (20).
10: **end if**
11: **Output**: $\gamma(\delta)$.
12: **for** $j = 1 : N_{\text{samples}}$ **do**
13: Sample uncertainty $\hat{\delta}_j$ according to $p(\delta)$.
14: Compute $\gamma(\hat{\delta}_j)$.
15: **end for**
16: **Output**: probability distribution of bound on $\|y(T,\delta)\|_2$ (i.e., $\|y(T,\delta)\|_2 \leq \gamma(\delta)$).

5. APPLICATION: SPACECRAFT ATTITUDE AND ORBIT CONTROL SYSTEM

This section presents an approximated worst-case transient analysis of a spacecraft AOCS using the methodology in Section 4. A simplified model of an Earth observation satellite during a manoeuvre is used as an application case. The main boost engines are ignited, causing torques on the spacecraft that generate a transient response on the spacecraft attitude. The AOCS needs to counteract both manoeuvre-induced torques and environmental disturbances to keep the initial spacecraft attitude.

5.1 Model architecture

The simplified satellite model only considers rotational motion around one axis. The model consists of one central body (cb) that is considered as rigid and one solar array (sa) appendage that is treated as a flexible body. The attitude dynamics are modelled considering the inertias of both bodies linked via a torsional joint. These dynamics are represented through a linear, time-invariant model G_{SAT} in Fig. 1. The resulting state-space representation is defined by the state vector $x = [\varphi_{\text{cb}}\ \dot{\varphi}_{\text{cb}}\ \varphi_{\text{sa}}\ \dot{\varphi}_{\text{sa}}]$, with the rotation angle and rotation rate of the corresponding body φ_i and $\dot{\varphi}_i$, respectively. The plant input is the external torque τ_{cb} applied on the central body. The state-space representation of the system G_{SAT} is:

$$\begin{bmatrix} \dot{\varphi}_{\text{cb}} \\ \ddot{\varphi}_{\text{cb}} \\ \dot{\varphi}_{\text{sa}} \\ \ddot{\varphi}_{\text{sa}} \end{bmatrix} = \begin{bmatrix} 0 & 1 & 0 & 0 \\ -\frac{a_2}{J_{\text{cb}}} & -\frac{a_1}{J_{\text{cb}}} & \frac{a_2}{J_{\text{cb}}} & \frac{a_1}{J_{\text{cb}}} \\ 0 & 0 & 0 & 1 \\ \frac{a_2}{J_{\text{sa}}} & \frac{a_1}{J_{\text{sa}}} & -\frac{a_2}{J_{\text{sa}}} & -\frac{a_1}{J_{\text{sa}}} \end{bmatrix} \begin{bmatrix} \varphi_{\text{cb}} \\ \dot{\varphi}_{\text{cb}} \\ \varphi_{\text{sa}} \\ \dot{\varphi}_{\text{sa}} \end{bmatrix} + \begin{bmatrix} 0 \\ \frac{1}{J_{\text{cb}}} \\ 0 \\ 0 \end{bmatrix} \tau_{\text{cb}}$$
$$y = [1\ 0\ 0\ 0] \begin{bmatrix} \varphi_{\text{cb}} \\ \dot{\varphi}_{\text{cb}} \\ \varphi_{\text{sa}} \\ \dot{\varphi}_{\text{sa}} \end{bmatrix}, \tag{30}$$

with $a_1 = 2J_{\text{sa}}\xi_c\omega_c$, $a_2 = J_{\text{sa}}\omega_c^2$, being J_{cb} the inertia of the central body, J_{sa} the inertia of the solar array, ξ_c the flexible mode damping ratio, and ω_c the flexible mode angular frequency. Uncertainties in these 4 plant model parameters are considered in this paper and collected in Table 1, where each parameter is distributed uniformly within the limits given.

Table 1. Uncertain parameters

Param.	Nom. Value	Unit	Uncertainty
J_{cb}	12163	$\text{kg} \cdot \text{m}^2$	±20%
J_{sa}	97.8	$\text{kg} \cdot \text{m}^2$	±20%
ξ_c	0.001	-	±20%
ω_c	0.1257	rad/s	±20%

A feedback controller of order 8 is implemented in K in Fig. 1, where d represents the deterministic manoeuvre-induced torques and u the unknown environmental disturbances. In addition, a disturbance torque estimation/compensation is included through G_V and G_U of order 3 and 2, respectively. G_V estimates the rotation rate of the central body with φ_{cb}. G_U estimates the torque disturbance d using the estimated rotation rate from G_V and the actuated command.

The manoeuvre-induced torques are modelled as a constant disturbance torque of 15 $\text{N} \cdot \text{m}$ in d. This disturbance represents the torque induced on the spacecraft when the engines are actuated during the manoeuvre. In addition, unknown environmental disturbance torques are modelled through u via a $\mathcal{L}_2$-bounded input signal $\|u\|_{2,[0,T]} \leq 0.01$. This bound is obtained from nonlinear simulations of environmental models during the manoeuvre. The uncertain closed-loop model architecture of the analysis problem, with inputs d and u, output y, and order 17 is shown in Fig. 1. The uncertainty block $\Delta_{\text{SAT}} \in \mathbb{R}^{10\times10}$ captures the multiplicity of the plant uncertain parameters.

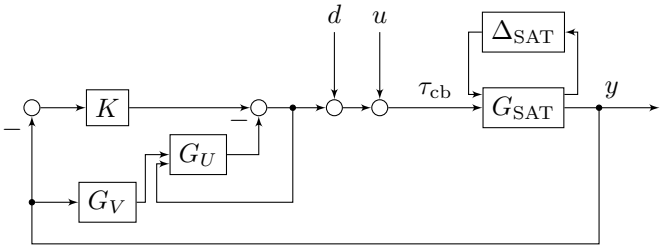

Fig. 1. Closed-loop model architecture

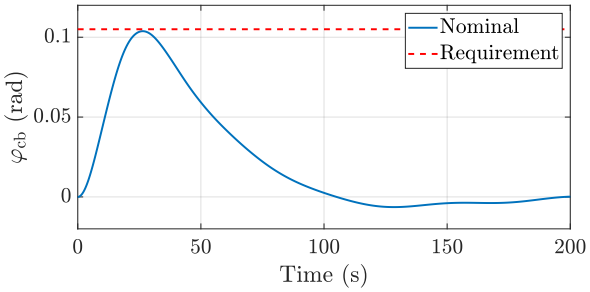

Fig. 2. Nominal attitude transient response

5.2 Transient performance analysis results

The objective is to assess the probability distribution of the bound on $\|y(T,\delta)\|_2$ of the uncertain system in Fig. 1, subject to the uncertainties described in Table 1, and the input torque disturbances d and u. The central body attitude φ_{cb} must stay within 0.105 rad during the entire manoeuvre. In a scenario with no uncertainties and no environmental disturbances, the nominal attitude transient response can be seen in Fig. 2. The bound on $\|y(T,\delta)\|_2$ is calculated for several times T to assess the impact of uncertainties and unknown disturbances on φ_{cb}. In this paper, the results for $T = 26$ s are presented as an example, since in the nominal case this time corresponds to the maximum overshoot.

The probabilistic worst-case transient analysis based on RDE and PCE described in Algorithm 1 will be used to assess the impact of uncertainties over the central body attitude. The Polynomial Chaos Expansion Toolbox (PoCET) for Matlab (Petzke et al. (2020)) is used to compute the projection integrals $\langle\cdot,\cdot\rangle$ in (16). The results presented in this paper are obtained for a second order polynomial expansion ($d_p = 2$) and $N_{samples} = 20{,}000$. Algorithm 1 results are compared to a Monte Carlo sampling campaign of (18) with the same number of PCE samples. The goal is to evaluate the accuracy and computational cost of this approach when the number of PCE samples is equivalent to that of Monte Carlo samples.

Results from both approaches (Algorithm 1 and Monte Carlo) are summarised in Table 2 and Fig. 3. Each of the approaches approximates the probability distribution of the bound on the absolute value of the central body attitude at time T. These two distributions are assessed through their mean and standard deviations, and the maximum sampled value is used to check requirement fulfilment. The histogram and cumulative probability functions in Fig. 3 are used to visualize the closeness between the two distributions.

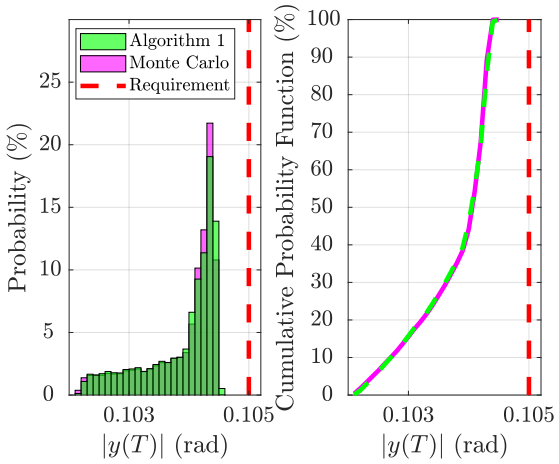

Fig. 3. Algorithm 1/Monte Carlo histogram and cumulative probability function comparison

Algorithm 1 is able to obtain an excellent approximation of the Monte Carlo distribution metrics as shown in Table 2 and Fig. 3. Moreover, the maximum value found after 20,000 samples stays below the requirement (0.105 rad). The main benefit of Algorithm 1 over Monte Carlo relies in the computational time, as shown in Table 3. Approximating the parameter-dependent RDE through PCE and then sampling it (Algorithm 1) is significantly faster than solving RDEs for sampled systems (Monte Carlo). For this application, Algorithm 1 achieves excellent results, 20 times faster then Monte Carlo, reducing the analysis time from almost 4 hours to around 11 minutes.

6. CONCLUSIONS

This paper presents a novel methodology to approximate worst-case transient performance of uncertain LTI systems, subject to both deterministic and $\mathcal{L}_2$-bounded inputs. This approach makes use of polynomial chaos expansion to approximate the probability distribution of the bound on the Euclidean norm of the system output. It is applied to a spacecraft attitude and orbit control system during a manoeuvre. Algorithm 1 offers significant computational benefits (factor of 20 faster) when compared to Monte Carlo, with negligible accuracy loss in the results.

ACKNOWLEDGEMENTS

The authors would like to thank Ralf Schubert and Catarina da Silva Lobo from Airbus Defence and Space GmbH for their valuable support, guidance, and feedback.

Table 2. Algorithm 1/Monte Carlo probability distribution metrics comparison

Method	Mean	Std. dev.	Max.
Algorithm 1	0.10387554 rad	0.000619 rad	0.10453 rad
Monte Carlo	0.10387553 rad	0.000620 rad	0.10451 rad
Rel. difference	$1.2 \cdot 10^{-5}$%	0.11%	0.02%

Table 3. Algorithm 1/Monte Carlo computational time comparison

Method	Computational time
Algorithm 1	$\sim$ 11 min
Monte Carlo	$\sim$ 3 h 40 min

REFERENCES

Althoff, D., Althoff, M., and Scherer, S. (2015). Online safety verification of trajectories for unmanned flight with offline computed robust invariant sets. In *2015 IEEE/RSJ International Conference on Intelligent Robots and Systems (IROS)*, 3470–3477. IEEE.

Biertümpfel, F., Theis, J., and Pfifer, H. (2023). Robustness analysis of nonlinear systems along uncertain trajectories. *IFAC-PapersOnLine*, 56(2), 5831–5836.

Biertümpfel, F. and Pfifer, H. (2018). Worst case gain computation of linear time-varying systems over a finite horizon. In *2018 IEEE Conference on Control Technology and Applications (CCTA)*, 952–957. IEEE.

Derollez, R. and Manchester, Z. (2020). Sample-based robust uncertainty propagation for entry vehicles. In *AAS/AIAA Astrodynamics Specialist Conference*.

Evangelisti, L.L. and Pfifer, H. (2022). Polynomial chaos approximation of the quadratic performance of uncertain time-varying linear systems. In *2022 American Control Conference (ACC)*, 1853–1858. IEEE.

Evangelisti, L.L. and Pfifer, H. (2024). Finite-horizon robustness analysis of an automatic landing system under probabilistic uncertainty. *Journal of Guidance, Control, and Dynamics*, 47(3), 464–472.

Farhood, M. (2024). Robustness analysis of uncertain time-varying systems with unknown initial conditions. *International Journal of Robust and Nonlinear Control*, 34(4), 2472–2495.

Green, M. and Limebeer, D.J. (1995). *Linear robust control*. Prentice-Hall, Inc.

Izquierdo Serra, M., Martin, M., Delchambre, S., Winkler, S., and Pfifer, H. (2025). Probabilistic verification of spacecraft acquisition sequence using polynomial chaos expansion. In *AIAA SCITECH 2025 Forum*. Orlando, FL, USA.

Marelli, S. and Sudret, B. (2015). Uqlab user manual–polynomial chaos expansions. Technical report, Chair of Risk, Safety & Uncertainty Quantification, ETH Zurich. Report UQLab-V0.9-104.

Moore, R.M. (2015). *Finite horizon robustness analysis using integral quadratic constraints*. Master's thesis, University of California, Berkeley, CA.

Petzke, F., Mesbah, A., and Streif, S. (2020). PoCET: a Polynomial Chaos Expansion Toolbox for Matlab. In *21st IFAC World Congress 2020*. Berlin, Germany.

Piprek, P. (2020). *Robust trajectory optimization applying chance constraints and generalized polynomial chaos*. Ph.D. thesis, Technische Universität München. doi: 10.13140/RG.2.2.17878.88649.

Schweidel, K.S., Buch, J.R., Seiler, P.J., and Arcak, M. (2020). Computing worst-case disturbances for finite-horizon linear time-varying approximations of uncertain systems. *IEEE Control Systems Letters*, 5(5), 1753–1758.

Sullivan, T.J. (2015). *Introduction to uncertainty quantification*, volume 63. Springer.

Thiele, F., Pfifer, H., and Biertümpfel, F. (2025). Finite-horizon robustness analysis under mixed disturbances using signal-IQCs. In *11th Symposium on Robust Control Design*. Porto, Portugal.

Wiener, N. (1938). The homogeneous chaos. *American Journal of Mathematics*, 60(4), 897–936.